Developmental differences in IFN signaling affect GATA1s-induced megakaryocyte hyperproliferation

Andrew J. Woo,[1] Karen Wieland,[1] Hui Huang,[1] Thomas E. Akie,[1] Taylor Piers,[1] Jonghwan Kim,[2] and Alan B. Cantor[1,3]

[1]Division of Pediatric Hematology-Oncology, Boston Children's Hospital/Dana-Farber Cancer Institute, Harvard Medical School, Boston, Massachusetts, USA. [2]Institute for Cellular and Molecular Biology, University of Texas, Austin, Texas, USA. [3]Harvard Stem Cell Institute, Cambridge, Massachusetts, USA.

About 10% of Down syndrome (DS) infants are born with a transient myeloproliferative disorder (DS-TMD) that spontaneously resolves within the first few months of life. About 20%–30% of these infants subsequently develop acute megakaryoblastic leukemia (DS-AMKL). Somatic mutations leading to the exclusive production of a short GATA1 isoform (GATA1s) occur in all cases of DS-TMD and DS-AMKL. Mice engineered to exclusively produce GATA1s have marked megakaryocytic progenitor (MkP) hyperproliferation during early fetal liver (FL) hematopoiesis, but not during postnatal BM hematopoiesis, mirroring the spontaneous resolution of DS-TMD. The mechanisms that underlie these developmental stage–specific effects are incompletely understood. Here, we report a striking upregulation of type I IFN–responsive gene expression in prospectively isolated mouse BM- versus FL-derived MkPs. Exogenous IFN-α markedly reduced the hyperproliferation FL-derived MkPs of GATA1s mice in vitro. Conversely, deletion of the α/β IFN receptor 1 (*Ifnar1*) gene or injection of neutralizing IFN-α/β antibodies increased the proliferation of BM-derived MkPs of GATA1s mice beyond the initial postnatal period. We also found that these differences existed in human FL versus BM megakaryocytes and that primary DS-TMD cells expressed type I IFN–responsive genes. We propose that increased type I IFN signaling contributes to the developmental stage–specific effects of GATA1s and possibly the spontaneous resolution of DS-TMD.

Introduction

Individuals with Down syndrome (DS) have a 10- to 20-fold higher overall risk of leukemia than do non-DS individuals (1–3). A substantial proportion of these excess cases is due to acute megakaryoblastic leukemia (DS-AMKL) during early childhood. DS-AMKL is often anteceded by a transient myeloproliferative disorder (TMD) in the neonatal period that is unique to DS (referred to herein as DS-TMD) and occurs in about 10% of DS newborns (4). The predominant hyperproliferative cells in DS-TMD exhibit erythromegakaryocytic features (5–7). DS-TMD shows a variety of clinical phenotypes, ranging from asymptomatic to respiratory distress and fulminant hepatic failure due to liver fibrosis (8). Strikingly, DS-TMD resolves spontaneously, typically within 2–3 months. However, in approximately 20%–30% of cases, DS-AMKL subsequently develops, often within 1–2 years after resolution of DS-TMD (8, 9).

Both DS-TMD and DS-AMKL cells harbor somatic mutations in the gene encoding GATA1, a key transcription factor involved in erythroid and megakaryocytic terminal maturation (10–15). Megakaryocyte (Mk) lineage-specific knockdown of GATA1 leads to impaired Mk maturation, excessive Mk proliferation, and marked thrombocytopenia in mice (16, 17). All DS-TMD and DS-AMKL *GATA1* mutations result in exclusive production of a short GATA1 isoform (GATA1s) that lacks the N-terminal 83 amino acids (10, 11). In some cases, multiple independent GATA1 mutations (all leading to exclusive GATA1s production) have been detected in stored newborn blood spots from DS children who developed DS-TMD and/or DS-AMKL, indicative of oligoclonal selection of GATA1s-containing progenitors during embryogenesis in DS individuals (13). GATA1s-producing mutations have not been identified in healthy individuals, DS-related acute lymphoblastic leukemia, or children with non–DS-AMKL, except for rare exceptions (18–20).

Knockin mice that exclusively produce GATA1s (referred to herein as GATA1s mice) have striking developmental stage–specific defects in Mk growth control (21). GATA1s Mks derived from yolk sac and E9.5–E14.5 fetal liver (FL) markedly hyperproliferate in vitro compared with WT Mks, whereas those derived from later embryonic stages or from newborn and adult BM proliferate close to normal, despite continued exclusive expression of GATA1s. These differences may account for the spontaneous resolution of DS-TMD in the early postnatal period.

The molecular basis for the stage-specific effects of GATA1s on Mk hyperproliferation remains largely unknown. 2 models could explain these findings: (a) the existence of a unique, transient population of megakaryocytic progenitor cells (MkPs) during yolk sac and early FL hematopoiesis that are selectively sensitive to the effects of GATA1s; and/or (b) developmental differences in the microenvironment that influence the effect of GATA1s on Mk proliferation.

In order to gain insight into these potential differences (either model), we compared global gene expression profiles of prospectively isolated murine early FL–derived (E13.5) and adult BM–derived MkPs (FL-MkPs and BM-MkPs, respectively). This revealed a number of critical differences between these 2 populations in WT and GATA1s mice, particularly in the expression of type I IFN–

Authorship note: Andrew J. Woo and Karen Wieland contributed equally to this work.

Conflict of interest: The authors have declared that no conflict of interest exists.

Citation for this article: *J Clin Invest.* 2013;123(8):3292–3304. doi:10.1172/JCI40609.

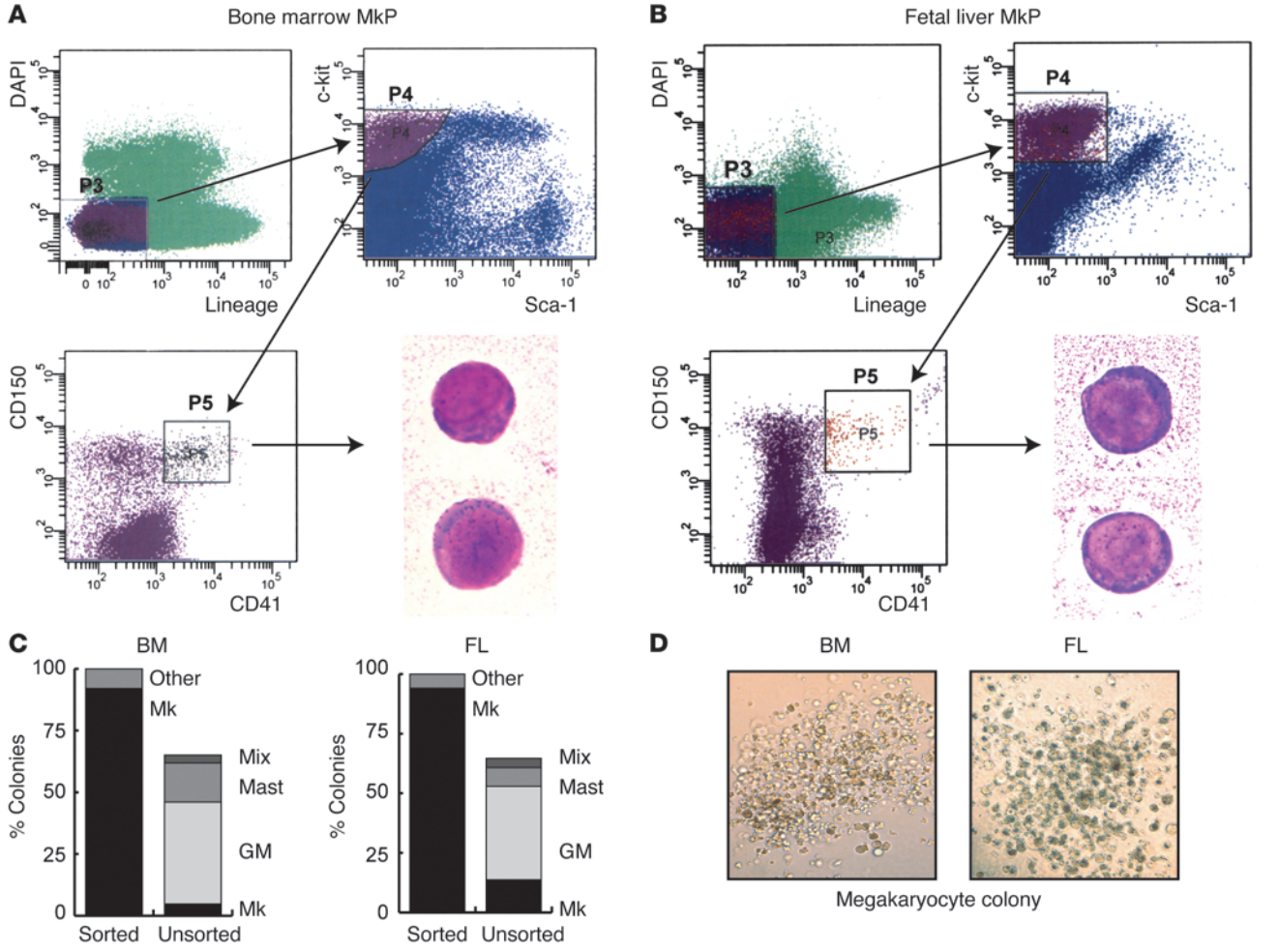

Figure 1

Flow cytometric sorting of MkPs from adult BM and E13.5 FL. (**A** and **B**) FACS plots and gates used for cell sorting. Cells were stained with antibodies against lineage markers, c-KIT, Sca-1, CD41, and CD150. Dead cells were identified by staining with DAPI and were excluded. May-Grünwald-Giemsa stains of cytospun freshly sorted BM and FL MkPs are also shown (original magnification, ×1,000). (**A**) Percent BM-MkPs gated relative to the starting population was as follows: P3, 17%; P4, 16.5%; P5, 1.9%. (**B**) Percent FL-MkPs gated relative to the starting population was as follows: P3, 38.2%; P4, 24.4%; P5, 1.2%. (**C**) Colony-forming assays. Percentage of colony type from sorted or unsorted BM and FL cells cultured in semisolid medium (after red blood cell lysis) containing TPO, erythropoietin, stem cell factor, IL-3, IL-11, and GM-CSF. Colonies were enumerated after 8 days. Cell accumulations of 3 or more cells were considered a colony. (**D**) Representative Mk colonies (unstained) from BM (day 7 of culture) or FL (day 8 of culture). Original magnification, ×100.

responsive genes. We provide evidence that increased type I IFN signaling during Mk ontogeny contributes to the developmental stage–specific effects of GATA1s on Mk proliferation.

Results

Prospective isolation of FL-MkPs and BM-MkPs. Since culturing of MkPs from FL or BM could potentially alter important gene expression differences, we performed our analysis directly on fluorescence-activated cell sorted (FACS) MkPs. E13.5 was chosen as a gestational time point to assess FL-MkPs, since the hyperproliferative phenotype of GATA1s Mks is apparent at this stage (21). We began our studies with WT mice since the developmental stage–specific hyperproliferation of FL-MkPs from GATA1s mice might confound the initial gene expression analysis. Pronk et al. reported that the immunophenotype $Lin^-Sca\text{-}1^-c\text{-}KIT^+CD150^+CD41^+$ greatly enriches for committed MkPs from mouse BM (22). We used this set of cell surface markers to isolate MkPs from WT E13.5 mouse FL and adult BM (Figure 1, A and B). There were no significant morphologic differences based on May-Grünwald-Giemsa staining between cells sorted from FL versus BM (Figure 1, A and B). Culturing of the sorted cell populations in semisolid media containing cytokines supporting multilineage growth showed that greater than 95% of sorted cells derived from both sources gave rise to pure Mk colonies (Figure 1C). The unsorted starting population gave rise to multiple colony types, as expected. There were subtle morphological differences between Mk colonies derived from FL-MkPs versus BM-MkPs, with the former appearing somewhat larger and more light refractive than the latter (Figure 1D), although the significance of this remains uncertain. These findings indicate that the immunophenotype $Lin^-Sca\text{-}1^-c\text{-}KIT^+CD150^+CD41^+$ markedly enriches for FL-MkPs similar to that reported for BM-MkPs and that there was minimal contamination with myeloid progenitor cells in our sorted samples.

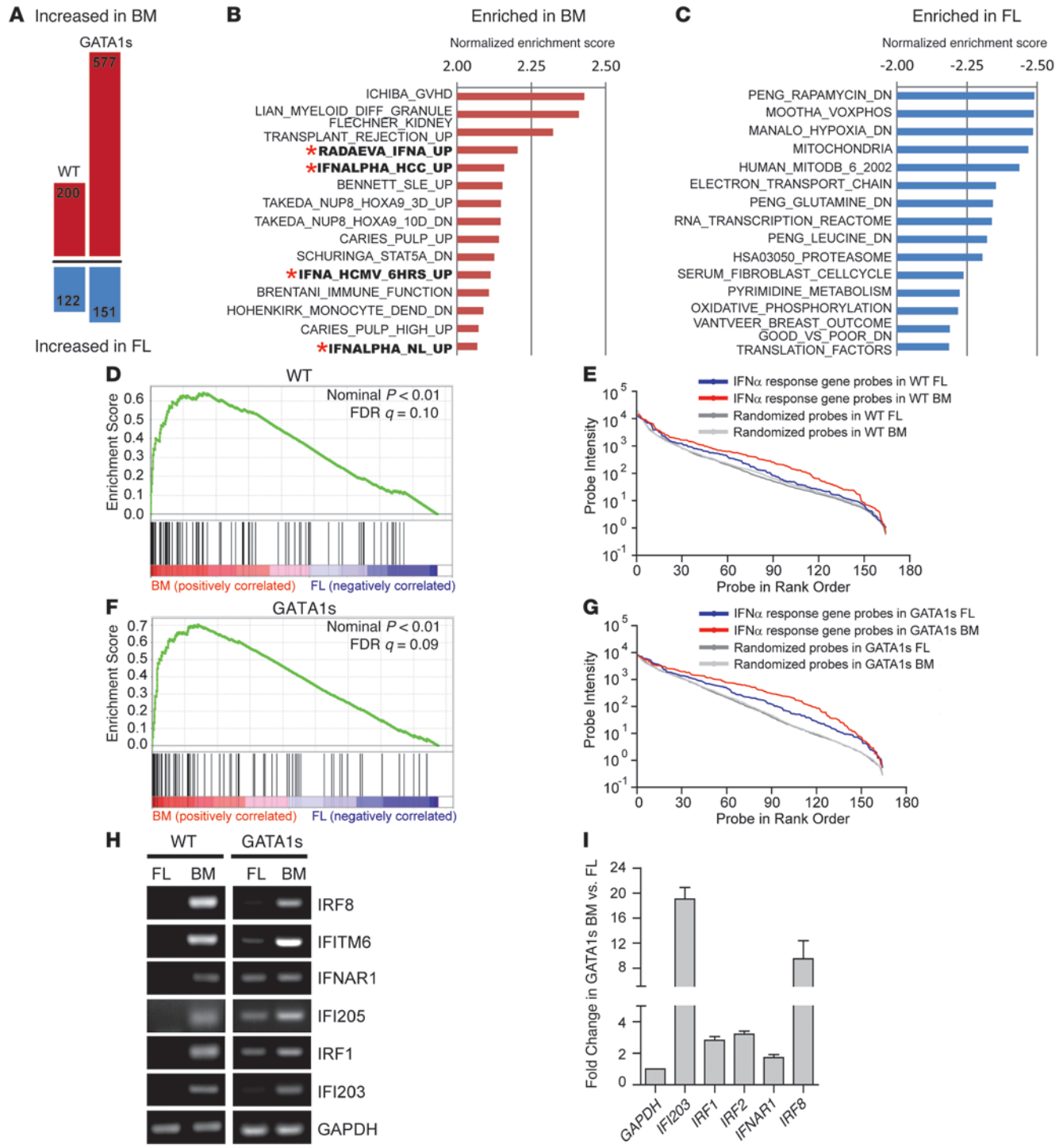

Figure 2

Gene expression analysis of FL-MkPs versus BM-MkPs. (**A**) Total number of genes whose expression changed >4-fold with $P < 0.05$ among the 3 biologic replicates and were represented by probes on the array comparing FL-MkPs versus BM-MkPs for male WT and GATA1s mice. (**B** and **C**) Analysis of gene sets enriched in BM-MkPs relative to FL-MkPs and vice versa from WT mice. Asterisks and bold type denote IFN-α–responsive gene sets. (**D** and **F**) GSEA for the combined set of 92 IFN-α–induced genes (Supplemental Table 3 and refs. 44, 45) compared with the differentially expressed genes in BM-MkPs versus FL-MkPs in WT (**D**) and GATA1s (**F**) mice. (**E** and **G**) Probe set intensities corresponding to each of the 92 genes, compared with intensities of 164 randomly selected probe sets, arranged from highest to lowest from the FL-MkP and BM-MkP datasets in WT (**E**) and GATA1s (**G**) mice. (**H** and **I**) Validation of differences in IFN-α–responsive gene expression in FL-MkPs versus BM-MkPs by conventional PCR (**H**) and qRT-PCR (**I**). Some lanes in **H** were run on different gels or noncontiguous lanes of the same gel.

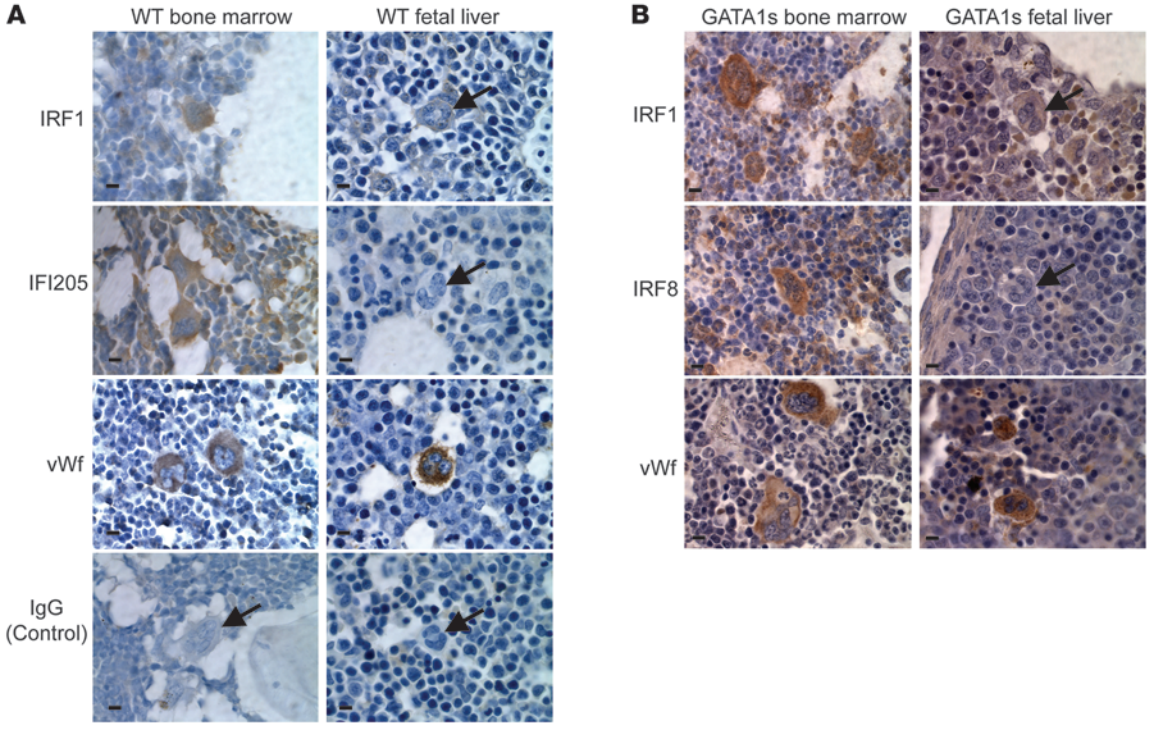

Figure 3
Increased protein levels of type I IFN–responsive genes in BM versus FL Mks. (**A**) In situ immunohistochemical staining for IRF1 and IFI205 in adult femur BM and E13.5 FL of WT mice. Staining for vWF served as a positive control for Mks. Positive staining appears brown; counterstain is blue. Arrows indicate Mks. See also Supplemental Figure 3. (**B**) In situ immunohistochemical staining for IRF1 and IRF8 in GATA1s male mice. Staining for vWF is indicated as a positive control. See also Supplemental Figure 4. Scale bars: 5 μm.

Upregulation of IFN-α/β–inducible genes in FL-MkPs and BM-MkPs. Global gene expression of the FACS-sorted populations was then examined by cDNA microarray analysis. Total RNA was extracted from 20,000 freshly sorted FL-MkPs and BM-MkPs, amplified, reverse transcribed, and hybridized to Affymetrix 430 2.0 oligonucleotide microarrays. These gene chips contain about 45,000 probe sets, allowing for interrogation of more than 34,000 well-characterized genes. The cDNA microarray analysis was performed in triplicate using 3 independent cell harvests and sorts.

We first examined the expression of several key Mk transcription factors and cytokine receptor genes, including *Gata1*, *Gata2*, *Fog1*, *Fli1*, *Gabpa*, *Runx1*, and *Mpl* (Supplemental Figure 1; supplemental material available online with this article; doi:10.1172/JCI40609DS1). Transcript levels for all of these genes were considerably above background, confirming our selection of Mk-committed cells by the FACS sorting procedure. The expression differences between FL-MkPs and BM-MkPs were all relatively small, the largest being about a 1.8-fold increase of *Gata2* mRNA and a 2-fold decrease of *Gata1* mRNA in BM-MkPs compared with FL-MkPs.

We next examined the dataset more globally. After filtering for genes having at least a 4-fold change in expression level and $P < 0.05$ (see Methods), there were 200 upregulated and 122 downregulated genes in BM-MkPs versus FL-MkPs (Figure 2A and Supplemental Tables 1 and 2). Gene Ontology (GO) analysis showed enrichment for genes associated with immune function in BM-MkPs and mitochondrial/metabolism function in FL-MkPs (Supplemental Figure 2, A and B). Gene set enrichment analysis (GSEA) using all available curated gene sets revealed striking enrichment for IFN-α–responsive genes in BM-MkPs versus FL-MkPs (Figure 2B and Supplemental Figure 2E). There was also significant enrichment for genes induced by the other type I IFN, IFN-β (Supplemental Figure 2F), which signals through the same receptor as IFN-α. Gene sets involved in metabolism and mitochondrial function were enriched in FL-MkPs versus BM-MkPs (Figure 2C). Given the known potent antiproliferative effects of IFN-α on Mk growth (23) and the clinical response of myeloproliferative disorders to IFN-α treatment (24–26), we chose to focus the remainder of the current study on the type I IFN signaling pathway.

After combining the 4 different publicly available IFN-α–induced gene sets shown in Figure 2B and eliminating duplicate genes, we generated a more comprehensive list of 92 IFN-α–induced genes (Supplemental Table 3). GSEA using the 92-gene list demonstrated significant enrichment in BM-MkPs compared with FL-MkPs (false discovery rate [FDR], 0.10; nominal $P < 0.01$; Figure 2D). A plot of the normalized signal intensities of the 164 probes corresponding to these 92 genes compared with the average intensity of 164 randomly selected probes is shown in Figure 2E.

We validated the differences in selected gene expression by quantitative real-time RT-PCR (qRT-PCR) from independently harvested/sorted cells. However, the signals from the FL-MkPs were so low for many of the genes that meaningful numbers could not be generated. Figure 2H shows an ethidium bromide–stained gel of the PCR products for a more qualitative analysis. Quantitative analysis of IFN-α/β receptor 1 (IFNAR1), 1 of the 2 IFNAR subunits, showed about 1.5-fold higher expression in BM-MkPs than FL-MkPs (data not shown).

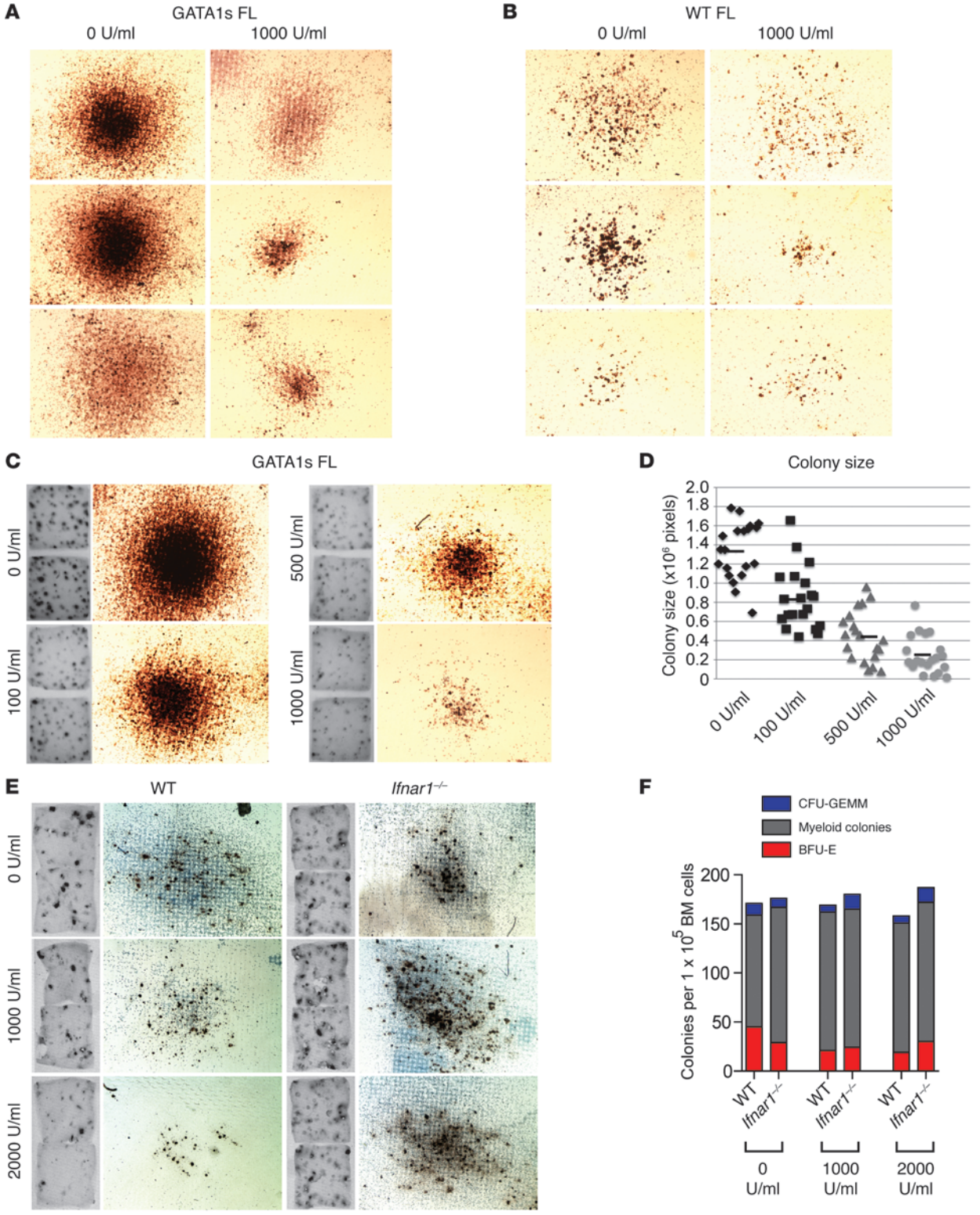
A
GATA1s FL
0 U/ml
1000 U/ml
B
WT FL
0 U/ml
1000 U/ml
C
GATA1s FL
0 U/ml
100 U/ml
500 U/ml
1000 U/ml
D
Colony size
Colony size (x10^6 pixels)
2.0
1.8
1.6
1.4
1.2
1.0
0.8
0.6
0.4
0.2
0
0 U/ml
100 U/ml
500 U/ml
1000 U/ml
E
WT
Ifnar1−/−
0 U/ml
1000 U/ml
2000 U/ml
F
CFU-GEMM
Myeloid colonies
BFU-E
Colonies per 1 x 10^5 BM cells
200
150
100
50
0
WT
Ifnar1−/−
WT
Ifnar1−/−
WT
Ifnar1−/−
0 U/ml
1000 U/ml
2000 U/ml

Figure 4
Antiproliferative activity of IFN-α on GATA1s-containing E13.5 FL Mks. (**A** and **B**) Representative CFU-Mk colony morphologies from male GATA1s or WT E13.5 FL cultured with 5 ng/ml TPO and 0 or 1,000 U/ml recombinant murine IFN-α. Colonies were fixed and stained for AChE activity after 7 (GATA1s) or 8 (WT) days. Original magnification, ×40. (**C**) AChE stained CFU-Mk colonies generated from male GATA1s E13.5 FL cultured with 5 ng/ml TPO and 0, 100, 500, or 1,000 U/ml recombinant IFN-α. Original magnification, ×40. Images of the entire slides are shown at left. (**D**) Effect of IFN-α treatment on CFU-Mk colony size from GATA1s E13.5 FL cultured in the presence of 5 ng/ml TPO and the indicated concentrations of IFN-α. Colony size is given as the number of pixels encompassing the entire colony after photographing the culture dishes (see Methods). Horizontal bars denote means. (**E**) Relative lineage-selective effects of IFN-α on Mk growth. Shown are representative BM AChE-stained CFU-Mk colonies from WT or *Ifnar1*$^{-/-}$ mice cultured in the presence of 5 ng/ml TPO and the indicated IFN-α concentrations. Original magnification, ×40. Images of the entire slides are shown at left. (**F**) Quantitation of BFU-E, CFU-GM, and CFU-GEMM of separate cultures grown in MethoCult (Stem Cell Technologies) semisolid medium containing SCF (50 ng/ml), IL-3 (10 ng/ml), IL-6 (10 ng/ml), EPO (3 IU/ml), insulin (10 μg/ml), transferrin (200 μg/ml), and the indicated IFN-α concentrations. See also Supplemental Figure 5.

Developmental stage–specific differences in type I IFN–inducible gene expression in GATA1s mice. In order to determine whether the differences we observed in the WT mice are preserved in the setting of exclusive GATA1s production, MkP isolation and gene expression analysis were repeated using GATA1s mice (21). Numerous genes were differentially expressed between BM-MkPs and FL-MkPs of GATA1s mice, with 577 genes upregulated and 151 genes downregulated greater than 4-fold ($P < 0.05$; Figure 2A). As expected, GO analysis of highly expressed genes in FL-MkPs versus BM-MkPs showed significant enrichment for mitosis-related genes (Supplemental Figure 2D). However, significant enrichment for IFN-α– and IFN-β–responsive gene sets was still apparent in BM-MkPs versus FL-MkPs, similar to the results obtained from WT mice (Figure 2F and Supplemental Figure 2, C, E, and G). Although the GATA1s FL-MkPs expressed these genes at relatively higher levels than WT FL-MkPs, there was still a significant increase comparing GATA1s BM-MkPs and FL-MkPs (FDR, 0.09; nominal $P < 0.01$; Figure 2, G–I).

Differential protein levels of type I IFN–responsive genes in BM versus FL Mks. In situ immunohistochemistry was performed next to confirm the differences in protein expression of type I IFN–responsive genes in Mks. As shown in Figure 3A and Supplemental Figure 3, we observed marked staining of Mks in WT adult BM for both IRF1 and IFI205. In contrast, only background staining was apparent in morphologically recognizable Mks from E13.5 FL. Similar differences in IRF1 and IRF8 protein levels were observed in GATA1s mouse BM versus FL Mks (Figure 3B and Supplemental Figure 4). Staining for the Mk marker protein vWF was strongly positive in both BM and FL samples. We conclude that murine BM-MkPs/BM Mks have substantial upregulation of type I IFN–inducible genes compared with E13.5 FL-MkPs/FL Mks and that this also occurs in a GATA1s genetic background.

Exogenous IFN-α inhibits hyperproliferation of GATA1s-containing Mks. If increases in type I IFN–responsive gene expression were an important determinant of the stage-specific effects of GATA1s on Mk hyperproliferation, then culturing of early GATA1s FL-MkPs with a type I IFN would be expected to counteract their hyperproliferative phenotype. To test this, single-cell suspensions were prepared from E13.5 FL from GATA1s or control WT mice and cultured in collagen-based semisolid media containing thrombopoietin (TPO) and increasing concentrations of IFN-α. As previously described (21), GATA1s Mks markedly hyperproliferated compared with WT Mks in the presence of TPO alone; however, their hyperproliferation was markedly attenuated in a dose-dependent manner when IFN-α was included (Figure 4, A, C, and D). IFN-α also limited the proliferation of WT E13.5 FL Mks, as expected (23), but the effects were not as pronounced as for GATA1s Mks (Figure 4B).

The antiproliferative effects of IFN-α were relatively selective for the Mk lineage. Colony number and size for adult BM myeloid (CFU-G, CFU-M, and CFU-GM) and mixed myeloid (CFU-GEMM) were only slightly affected at the doses used, in contrast to the marked effect on CFU-Mk (Figure 4, E and F, and Supplemental Figure 5). BFU-Es were also modestly reduced (Figure 4F). As expected, CFU-Mks and BFU-Es from mice lacking IFNAR1 (27) were not affected by IFN-α treatment (Figure 4, E and F, and Supplemental Figure 5).

Delayed resolution of GATA1s Mk hyperproliferative phenotype in the absence of IFN-α/β signaling. Our model also predicted that loss of IFN-α/β signaling in the postnatal BM environment would abrogate or delay resolution of the developmental stage–specific hyperproliferation of GATA1s MkPs. To test this, GATA1s mice were bred to *Ifnar1*$^{-/-}$ mice. The resulting compound *Ifnar1*$^{-/-}$::GATA1s mice were born at the expected Mendelian ratio. We first examined the peripheral blood counts of these mice at 3–4 weeks of age. Male *Ifnar1*$^{-/-}$ mice and hemizygous GATA1s mice (*GATA1* is located on the X chromosome) had platelet counts similar to those of C57BL/6 WT controls. However, *Ifnar1*$^{-/-}$::GATA1s male mice had significantly lower platelet counts ($624 \times 10^9 \pm 20 \times 10^9$ platelets/l; $n = 10$) than male WT ($838 \times 10^9 \pm 27 \times 10^9$ platelets/l; $n = 10$), *Ifnar1*$^{-/-}$ ($812.7 \times 10^9 \pm 30 \times 10^9$ platelets/l; $n = 10$), or GATA1s ($790 \times 10^9 \pm 18 \times 10^9$ platelets/l; $n = 10$) littermate controls ($P < 0.05$, 2-tailed Student's t test; Figure 5A). They also had larger mean platelet volumes (Figure 5B). In contrast, there were no significant differences in red blood cell or total white blood cell counts (Figure 5, C and D). Thus, a genetic interaction exists between GATA1s and IFNAR1 with regard to thrombopoiesis.

We next examined the proliferation status of BM-MkPs from 3- to 4-week-old mice. CFU-Mk colony assays showed significantly larger Mk colony size in male *Ifnar1*$^{-/-}$::GATA1s mice compared with male WT, *Ifnar1*$^{-/-}$, or GATA1s mice (Figure 5, E–I). As previously described (21), Mk colonies from GATA1s mice contained a large number of acetylcholinesterase-negative (AChE$^-$) cells, with scattered AChE$^+$ cells mixed in, suggesting an expansion of more immature Mks in these cultures. There was an exaggerated number of AChE$^-$ cells in the base of *Ifnar1*$^{-/-}$::GATA1s colonies (Figure 5H), which suggests expansion of the more immature Mk cells. In vivo BrdU incorporation analysis confirmed the higher proliferative rate of CD41$^+$ cells in *Ifnar1*$^{-/-}$::GATA1s compared with WT, *Ifnar1*$^{-/-}$, and GATA1s mice (Figure 5, J and K).

As an independent means to test our model, we acutely inhibited IFN-α/β signaling in 4- to 6-week-old mice by intraperitoneal injection of neutralizing IFN-α and IFN-β antibodies (Figure 6A). WT mice showed only a minimal increase in the percentage of BM CD41$^+$forward scatter^{hi} cells (i.e., Mks) 8 days after injec-

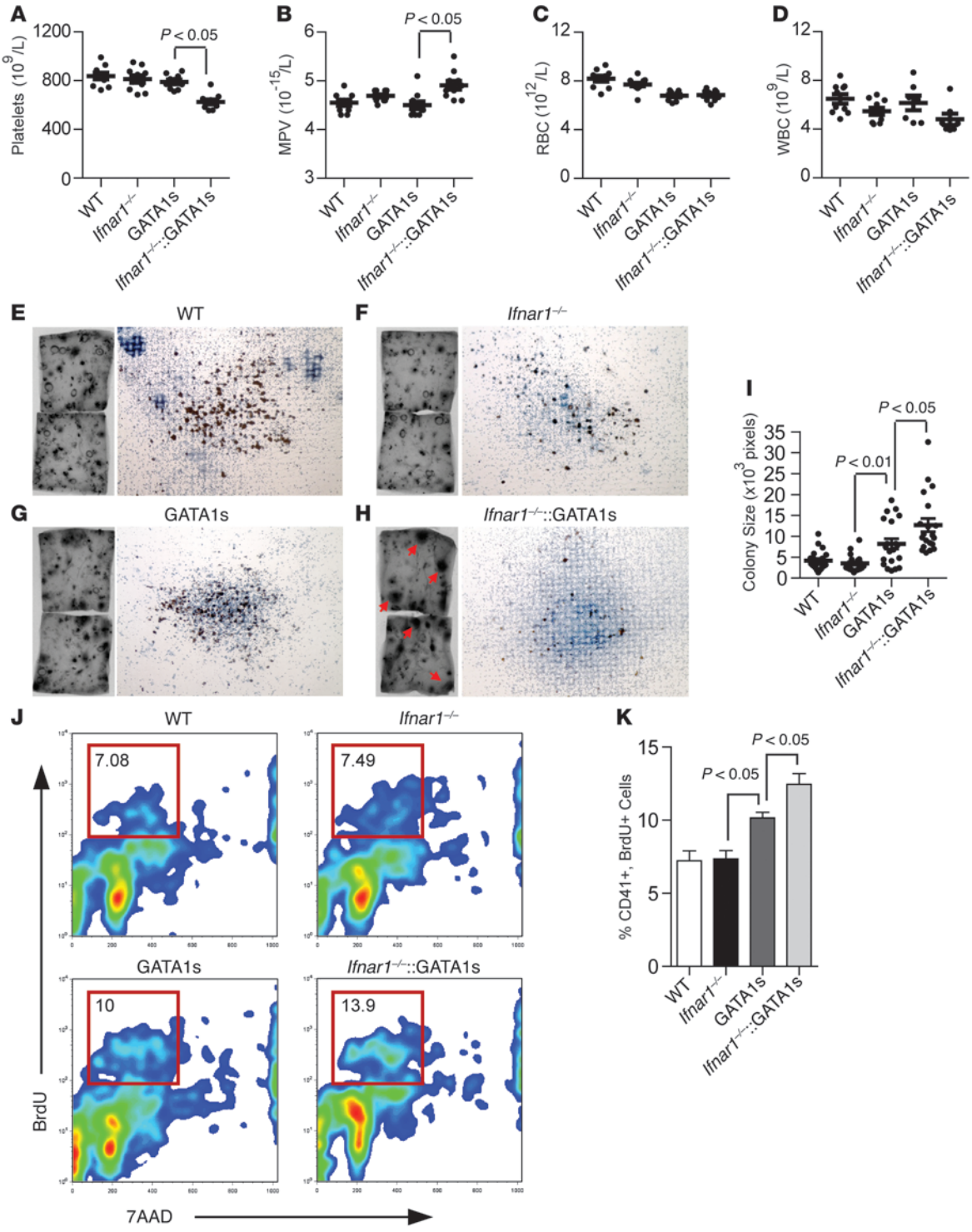

Figure 5

Enhanced postnatal proliferation of GATA1s-containing Mks in an *Ifnar1*$^{-/-}$ genetic background. (**A**–**D**) Peripheral blood platelet count (**A**), mean platelet volume (**B**), red blood cell count (**C**), and white blood cell count (**D**) of WT (C57BL/6), *Ifnar1*$^{-/-}$, GATA1s, and *Ifnar1*$^{-/-}$::GATA1s male mice at 3–4 weeks of age. (**E**–**H**) Representative AChE-stained BM CFU-Mk colonies from each mouse genotype at 3–4 weeks of age. Original magnification, ×40. Images of the entire slides are shown at left. Red arrows in **H** indicate hyperplastic colonies. (**I**) Quantitation of colony size (mean number of pixels covered by colonies derived from photographs) from 20 randomly selected colonies. (**J**) Representative flow cytometry plots for BrdU and 7AAD (DNA content stain) of CD41$^+$ gated cells obtained from the BM of 3- to 4-week-old mice of the indicated genotypes. (**K**) Percent CD41$^+$BrdU$^+$ cells from **J** (n = 3).

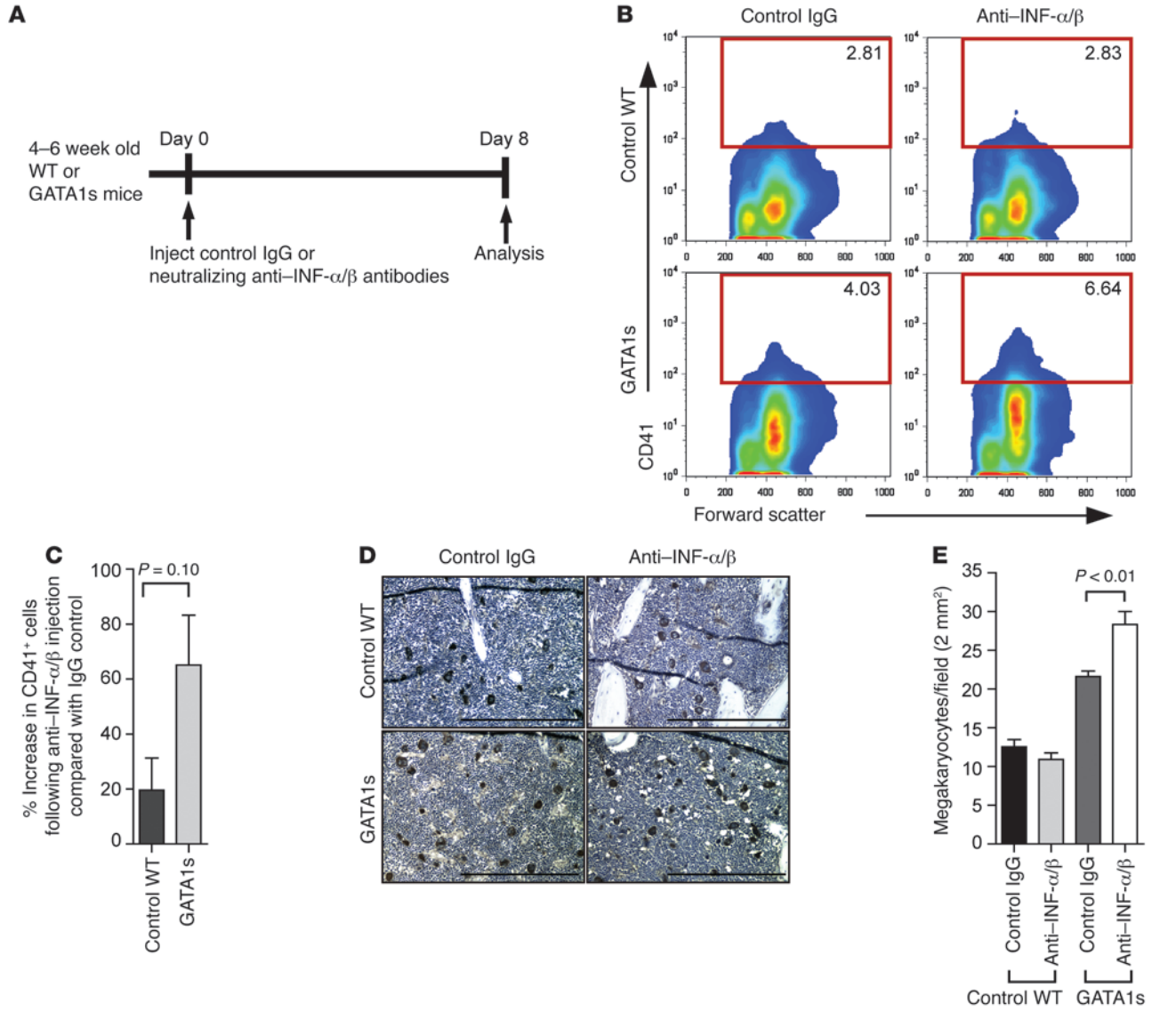

Figure 6

Expansion of BM Mks in GATA1s mice injected with neutralizing IFN-α/β antibodies. (**A**) Experimental scheme. 4- to 6-week-old GATA1s or age-matched WT mice were injected intraperitoneally with 1 × 10^4 neutralizing units of anti–IFN-α and anti–IFN-β antibodies each, or an equivalent amount of normal rabbit IgG. 8 days after injection, animals were euthanized, and BM was harvested. (**B**) Flow cytometric color-contour plots for CD41 staining and forward scatter from whole BM (after red blood cell lysis) from 1 representative experiment. (**C**) Change in CD41$^+$ cell frequency in mice injected with neutralizing IFN-α/β antibodies versus control IgG (n = 3). Results of 3 independent experiments are shown. (**D**) Representative vWF immunohistochemical stained sections of femur BM from mice injected 8 days earlier with neutralizing anti–IFN-α/β antibodies or equivalent amounts of control IgG. Scale bar: 1 mm. (**E**) Quantitation of the data in **D**, showing the mean number of Mks per 2-mm^2 field in 10 randomly selected sections.

tion compared with control mice that received an equivalent amount of control IgG (19.6% ± 6.8%; n = 3; Figure 6, B and C). GATA1s mice receiving control IgG had a higher percentage of CD41$^+$forward scatter^{hi} cells at baseline than WT mice injected with IgG, consistent with low-level hyperproliferation of GATA1s Mks even in the postnatal period at this age. However, there was an additive increase of CD41$^+$forward scatter^{hi} BM cells in GATA1s mice after injection of the neutralizing IFN-α/β antibodies (65% ± 10.5% versus control IgG; n = 3; Figure 6C), indicative of their proliferative sensitivity to low IFN-α/β signaling. Enumeration of BM Mks in situ by vWF immunohistochemical staining showed similar results (Figure 6, D and E). We conclude that IFN-α/β signaling normally dampens the hyperproliferative phenotype of GATA1s Mks postnatally.

Role of IFN-α/β signaling in human Mk ontogeny. In order to determine whether the ontologic differences in Mk IFN-α/β signaling also apply to humans, we examined the expression of the IFN-α/β–responsive gene *IRF1* by in situ immunohistochemistry in FL from aborted fetuses (12- to 22-week estimated gestational age) versus postnatal BM (>1 year of age). Similar to the mouse studies, this experiment showed a marked increase in Mk IRF1 protein levels in BM versus FL, with no significant difference in vWF staining

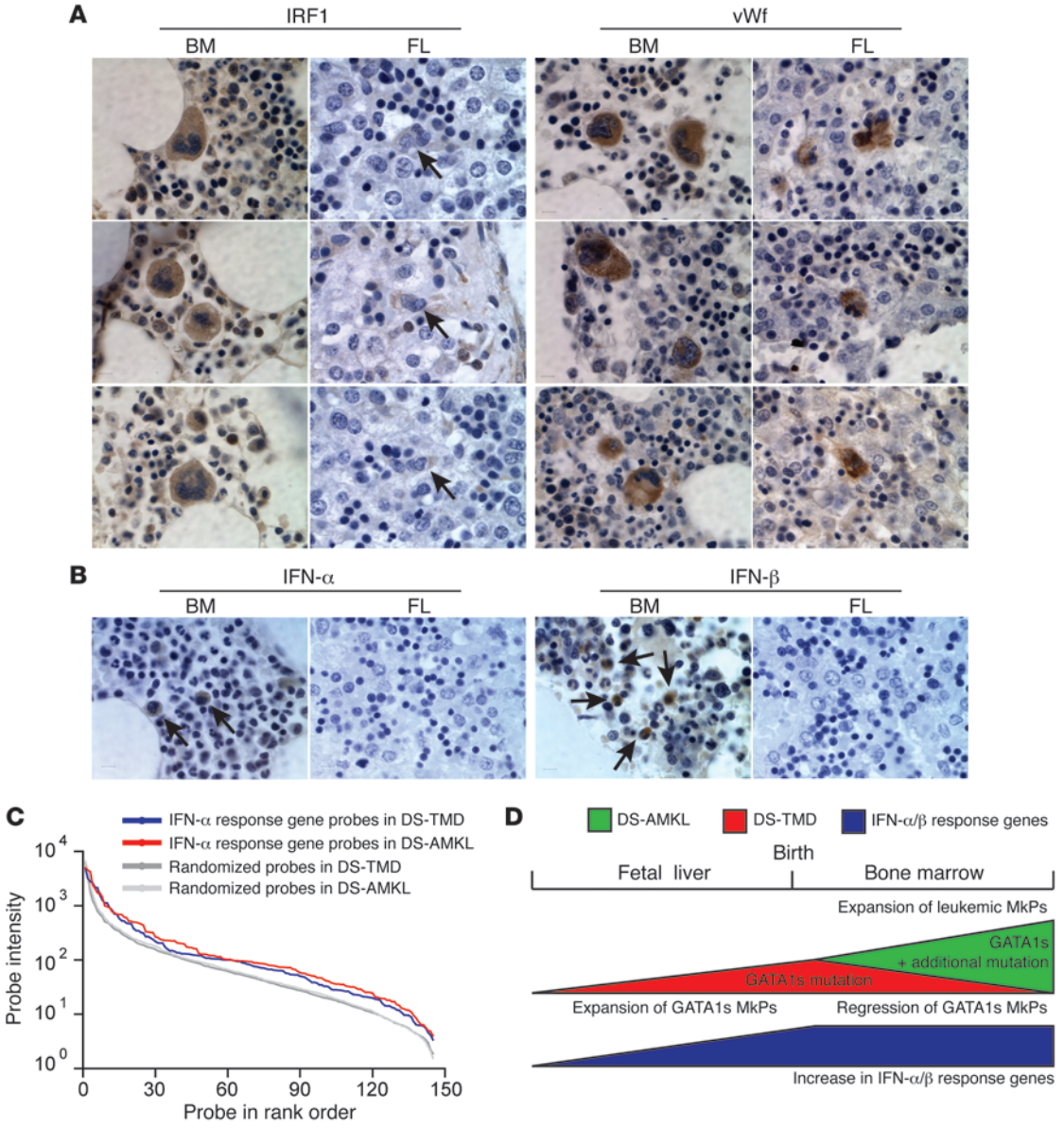

Figure 7

Developmental stage–specific difference in human Mk IFN-α–responsive gene expression. (**A**) In situ immunohistochemical staining for IRF1 and vWF in FL from 12- to 22-week estimated gestational age aborted human fetuses and from BM of >1-year-old individuals. Arrows indicate Mks. Original magnification, ×1,000. See also Supplemental Figure 6. (**B**) In situ immunohistochemical staining for IFN-α and IFN-β of human FL and BM as in **A**. Arrows indicate positive cells. Original magnification, ×1,000. See also Supplemental Figure 7. (**C**) Expression of IFN-α–responsive genes in human DS-TMD and DS-AMKL cells (based on data in ref. 6) compared with an equivalent number of randomly selected probes, shown in rank order. (**D**) Model for developmental stage–specific reduction in GATA1s-related Mk hyperproliferation with increases in IFN-α/β–responsive gene expression.

(Figure 7A and Supplemental Figure 6). We also found cells staining for IFN-α and IFN-β in the BM, but not in FL samples (Figure 7B and Supplemental Figure 7). Thus, differences in IFN-α/β production in the BM versus FL microenvironment may account for the differences in type I IFN–induced gene expression and their effects on GATA1s-induced MkP hyperproliferation.

Type I IFN signaling in human DS-TMD and DS-AMKL. Finally, we analyzed previously reported gene expression profiles of DS-TMD and DS-AMKL primary cells (6) using the human equivalent of the 92 IFN-α–induced gene panel described above (Supplemental Table 3). These samples represent mixtures of postnatal peripheral blood and BM-derived specimens. FL samples were not available for comparison. Nonetheless, the DS-TMD samples expressed IFN-α–responsive genes at levels considerably higher than background (Figure 7C), similar to our mouse postnatal BM-MkP data. This is consistent with their anticipated proliferative decline as the DS-TMD phase resolves. The DS-AMKL cells also expressed IFN-α–responsive genes a levels higher than background (Figure 7C). We speculate that additional genetic events in DS-AMKL cells allow them to escape the antiproliferative effects of type I IFN signaling.

Discussion

Our findings indicated that key developmental stage–specific differences exist between early FL-MkPs and adult BM-MkPs with respect to type I IFN–responsive gene expression. Moreover, we showed that FL-MkPs with exclusive production of the DS-TMD/DS-AMKL–associated GATA1s isoform lost their hyperproliferative phenotype when placed in an environment containing increased type I IFN signaling and that GATA1s-containing adult BM-MkPs partially reverted to a hyperproliferative phenotype upon loss of type I IFN signaling. These findings are consistent with type I IFN–responsive genes contributing to the stage-specific effects of GATA1s on Mk proliferation, and possibly to the spontaneous postnatal resolution of DS-TMD.

A trivial explanation for our gene expression findings would be that there was disproportionate contamination of the BM- versus FL-derived samples with other cell types that express type I IFN–responsive genes. Several pieces of evidence argue against this: (a) the colony assays performed on the sorted cells from both FL and BM produced >95% pure Mk colonies under conditions that supported multilineage growth, including myelomonocytic cells (Figure 1); (b) previous work showed that human $CD34^+$ in vitro–differentiated primary Mks express functional IFNAR1 and downstream type I IFN signaling pathway components (28); (c) the differential gene expression dataset from the BM versus FL samples did not show statistically significant enrichment for lymphocyte gene sets (data not shown); (d) in situ immunohistochemistry demonstrated that the different protein levels of type I IFN–responsive genes occurred within morphologically recognizable Mks (Figures 3 and 7); and (e) experimental manipulation of type I IFN signaling led to functional changes in GATA1s-containing cells (Figures 4–6). Thus, the differences in type I IFN–inducible gene expression we detected most likely occurs within the MkPs themselves.

Although IFN-responsive genes are well established for their role in antiviral responses, recent work suggests that they have broader roles in hematopoiesis. Xu et al. showed that the IFN response proteins IRF2 and IRF6 collaborate with GATA1 and the erythroid/megakaryocytic transcription factor SCL/TAL1 to specify active enhancers in adult versus fetal expressed erythroid genes in human $CD34^+$ cell–derived erythroid precursors (29). Matsuyama et al. reported that *Irf1*-knockout mice have deficient T cell development and that *Irf2*-knockout mice have ineffective BM hematopoiesis (30). Essers et al. demonstrated that IFN-α signaling activates dormant hematopoietic stem cells (31). Klimmeck et al. showed increased type I IFN–inducible protein abundance in prospectively isolated murine multipotent hematopoietic stem/progenitor cells ($Lin^-Sca\text{-}1^+c\text{-}KIT^+$) compared with myeloid committed progenitors ($Lin^-Sca\text{-}1^-c\text{-}KIT^+$) (32). Our present data provide additional evidence for broader roles of IFN-responsive genes in developmental hematopoiesis.

The increased expression of the type I IFN–responsive genes in BM-MkPs versus FL-MkPs raises the question of whether there are important microenvironmental differences that could account for this. Indeed, we were able to detect cells with IFN-α and IFN-β cytoplasmic immunostaining in BM, but not FL, samples. Prior studies have shown that osteoclasts and osteoblasts produce IFN-β (33, 34). As these cell types are present in the BM, but not the FL microenvironment, they could potentially account for some of the differences. We also examined for the presence of plasmacytoid dendritic cells, a major source of inducible IFN-α production, in early FL versus BM, but were not able to find reproducible quantitative differences (K. Wieland, T.E. Akie, and A.B. Cantor, unpublished observations). Further studies will be required to fully identify the complement of type I IFN–producing cells in these different hematopoietic niches.

Binding of IFN-α/β to its heterodimeric receptors, IFNAR1 and IFNAR2, leads to activation of the JAK-STAT pathway, with JAK1/TYK2 and STAT1/STAT2 being the most important contributors (35, 36). STAT1 expression is significantly downregulated in GATA1-deficient Mks (37), and enforced STAT1 or IRF1 expression partly rescues their maturation defects (38). *Stat1* mRNA transcript levels are also decreased in GATA1s versus WT Mks (21). Thus, a functional relationship exists between GATA1 and downstream IFN-α/β signaling pathway components. We propose that increased type I IFN signaling during ontogeny compensates for impaired STAT1 levels (and possibly additional defects) associated with exclusive GATA1s production in Mks, thereby leading to a developmental stage–specific reduction in the hyperproliferative phenotype (Figure 7D).

The hyperproliferation of adult GATA1s BM-MkPs in response to genetic or antibody-mediated inhibition of type I IFN signaling, while present, was not as robust as the marked hyperproliferation of GATA1s FL-MkPs. This suggests that additional mechanisms and/or pathways likely contribute to the developmental stage–specific effects of GATA1s on MkP hyperproliferation (and likely DS-TMD resolution). This could include IFN-γ signaling (which we also observed to be elevated in BM-MkPs relative to FL-MkPs), metabolic differences (Figure 2 and Supplemental Figure 2), IGF signaling (39), or mechanisms yet to be defined. Differences between human fetal and adult Mks have previously been noted, including smaller size, lower ploidy, and increased proliferative potential of FL Mks (40). Our expression datasets should provide a useful resource for further investigation of the developmental differences in megakaryopoiesis.

The antiproliferative effects of IFN-α are well established. It was first approved as an antiproliferative agent by the FDA in 1986 for the treatment of hairy cell leukemia. Since then, the range of applications has been extended to several other myeloproliferative diseases, such as polycythemia vera (24), essential thrombocytosis (25), and chronic myeloid leukemia (26). Recent pilot studies also suggest that it has efficacy in early-stage primary myelofibrosis (41). It has been used in neonates for the treatment of life-threatening hemangiomas that do not respond to corticosteroids. Currently, treatment of infants with life-threatening complications of DS-TMD involves the use of the chemotherapeutic agent Ara-C. Our results suggest that treatment with IFN-α may be beneficial in reducing the myeloproliferation in these cases, avoiding the need for cytotoxic agents. Whether reducing the burden of DS-TMD cells decreases the incidence of subsequent DS-AMKL is not currently known. However, if this is the case, our findings suggest that recombinant IFN-α may be a useful agent by which to achieve this. These questions will require further investigation.

In summary, our present results uncovered developmental stage–specific differences in type I IFN signaling during Mk ontogeny and provided evidence that they contribute to the developmental stage–specific effects of the GATA1s mutation on Mk hyperproliferation and possibly DS-TMD. Our findings also suggest that recombinant IFN-α could be explored as an alternative to Ara-C in the treatment of life-threatening DS-TMD.

Methods

Mice. GATA1s mice (21) were a gift from S. Orkin (Boston Children's Hospital, Boston, Massachusetts, USA). *Ifnar1*$^{-/-}$ mice (27) were a gift from G. Cheng (UCLA, Los Angeles, California, USA).

Purification of MkPs. BM cells were flushed from both femurs and tibias of adult C57BL/6 mice (3–8 months of age), and FL cells were harvested from E13.5 WT C57BL/6 embryos. To obtain MkPs, Lin$^-$Sca-1$^-$c-KIT$^+$CD41$^+$CD150$^+$ cells were isolated as previously described (22). Following red blood cell lysis, cells were preincubated with purified anti-mouse CD16/CD32 (BD Pharmingen) for 10 minutes on ice to inhibit nonspecific binding to Fc receptors. Cells were subsequently incubated 10 minutes with fluorochrome- or biotin-conjugated antibodies against lineage markers, Sca-1, c-KIT, CD41, and CD150. Staining with DAPI was used to exclude dead cells, and the MkPs isolated using an Aria FACS instrument (BD). All flow cytometry and FACS data were analyzed with FACSDiva software (BD).

Biotin-conjugated mouse lineage panel (CD3e, CD11b, CD45R/B220, Ly-6G and Ly-6C [Gr-1], Ter119/Ly-76), APC-conjugated streptavidin, PE/Cy7–conjugated Sca-1, and FITC-conjugated CD41 were purchased from BD Pharmingen. PerCp/Cy5.5–conjugated c-KIT and PE-conjugated CD150 were purchased from BioLegend. Cell morphology of freshly sorted cells was assessed after cytospin preparation and staining with May-Grünwald-Giemsa.

Colony-forming assays. For assessing purity of sorted MkPs, 1,000 FACS-sorted FL-MkPs or BM-MkPs or unsorted starting FL and BM populations were cultured in methylcellulose medium (MethoCult M3434; Stem Cell Technologies) containing 50 ng/ml SCF, 3.3 ng/ml GM-SCF, 10 ng/ml IL-3, 10 ng/ml IL-11, 2 IU/ml EPO, and 10 ng/ml TPO at 37°C, 5% CO_2, in a humidified chamber. Colonies were enumerated after 8–9 days using an inverted microscope (Leica DM IRB). Cell accumulations of 3 or more were considered a colony. Single colonies were picked and stained with May-Grünwald-Giemsa, benzidine (red blood cell specific), toluidine blue (mast cell specific), and acetylcholinesterase (Mk-specific stain) to confirm cell types.

For FL Mk colony assays, FL cells were obtained from E13.5 homozygous embryos of GATA1s mice (21). After harvesting, whole FL cells were kept on ice and rapidly brought into semisolid culture medium (MegaCult, Stem Cell Technologies). Cells were cultured for 7–8 days at 37°C, 5% CO_2, in an humidified environment with 5 ng/ml murine TPO and recombinant murine IFN-α (EMD Millipore; catalog no. IF009) in concentrations of 0, 100, 500, and 1,000 U/ml. Colonies were fixed in ice-cold acetone for 5 minutes, and AChE staining was performed according to the manufacturer's instructions. Experiments were performed in triplicate. Colony images were obtained with an upright microscope (Nikon eclipse e800; Nikon 4× CFI Plan Fluor lens, NA 0.13; room temperature; Photohead V-TP camera, multipoint sensor system; software, Spot advanced version 3.5.6 for Mac OS), and colony size was measured with image processing software (Photoshop CS3 extended; Adobe). Measurement was performed for 20 Mk colonies each — cultured in 5 ng/ml TPO, alone or with IFN-α (0, 100, 500, or 1,000 U/ml) — in a blinded fashion. WT FL cells were obtained at E13.5 from C57BL/6 mice and cultured as described for the GATA1s FL-MkPs, except that TPO was added to a final concentration of 20 ng/ml.

For BM Mk colony assays, mouse BM cells were cultured in Mega-Cult (Stem Cell Technologies) collagen-based semisolid medium with TPO (50 ng/ml), IL-6 (20 ng/ml), IL-11 (50 ng/ml), and IL-3 (10 ng/ml). Cultures were dried and stained for AChE as described for FL Mk cultures. For other BM hematopoietic colony assays, MethoCult (Stem Cell Technologies) semisolid medium containing SCF (50 ng/ml), IL-3 (10 ng/ml), IL-6 (10 ng/ml), EPO (3 IU/ml), insulin (10 μg/ml), transferrin (200 μg/ml), and IFN-α (0, 1,000, or 2,000 IU/ml) was used.

RNA extraction and microarray analysis. See Supplemental Methods.

Gene expression data analysis. Expression microarray data were analyzed using R and Bioconductor via Cistrome platform (42). Differential gene expression analysis was performed on Robust Multichip Average (RMA) normalized expression index. Limma regression method with a *P* value threshold of 0.05 was applied to derive the list of differentially expressed genes. GSEA (Broad Institute) was performed on MAS5 normalized microarray data (excluding rows with absent calls for all samples) (43). Gene sets used for the enrichment analysis were provided by the Broad Institute.

qRT-PCR. See Supplemental Methods.

Immunohistochemical staining. Mouse FLs from WT C57BL/6 E13.5 embryos were fixed in 4% paraformaldehyde for a minimum of 24 hours, then paraffin embedded and sectioned. Mouse adult BM was fixed in 4% paraformaldehyde for at least 24 hours, decalcified, paraffin embedded, and sectioned. Deparaffinized, rehydrated sections were preincubated in 0.3% Triton X-100 for 15 minutes at room temperature and immersed in 3% H_2O_2 for 5 minutes to block endogenous peroxidase activity. To retrieve Ifi205 antigens, samples were boiled in sodium-citrate buffer (1.8 mM citric acid, 8.2 mM sodium citrate, pH 6.0) for 30 minutes at 90°C and cooled down at room temperature for 20 minutes. vWF antigens were retrieved by incubation with proteinase K solution (pH 8) for 15 minutes at 37°C and 15 minutes at room temperature. IRF1 staining did not require antigen retrieval. Endogenous avidin expression was blocked with an avidin/biotin complex according to the manufacturer's instructions (avidin/biotin blocking kit; Vector Laboratories). Nonspecific binding was inhibited by preincubation with 10% goat (Vector Laboratories) blocking solution, and sections were incubated overnight at 4°C with primary antibodies diluted in PBS (Ifi205, diluted 1:500; gift of J. Keller, National Cancer Institute, Frederick, Maryland, USA), vWF (polyclonal rabbit, diluted 1:500; DAKO), and IRF1 (M-20, diluted 1:100; Santa Cruz Biotechnology, sc-640). Negative controls were processed in parallel, except that PBS was substituted for the primary antibody. After washing 3 times, secondary antibody incubation was performed for 30 minutes at room temperature using biotinylated goat anti-rabbit IgG (Vector Laboratories) diluted 1:500 (vWF and Ifi205) or 1:200 (IRF1 and negative control) in PBS. HRP activity of biotin-labeled tissue antigens was achieved by incubation with ABC-HRP (Vectastain Elite ABC kit; Vector Laboratories) for 30 minutes, after which HRP activity was revealed with DAB (DAB substrate kit for peroxidase; Vector Laboratories) for 30–60 seconds. Finally, sections were counterstained and mounted.

Immunohistochemical staining of GATA1s mouse FL and BM was as described for WT animals, except that 10% formalin was used instead of paraformaldehyde. The human FL samples were obtained from 12- to 22-week estimated gestational age fetuses that were aborted due to a variety of causes, including tetralogy of Fallot, hypoplastic left heart, and neural tube defects. BM biopsy material was obtained as excess material from subjects over 1 year of age undergoing restaging BM studies after treatment for a variety of solid cancers. Human samples were fixed in Bouin's solution. To retrieve vWF, IRF1, IRF8, IFN-α, and/or IFN-β antigens for human and/or GATA1s mouse samples, sections were boiled in sodium-citrate buffer. Endogenous peroxidase activity was blocked using 3% H_2O_2 for 20 minutes along with endogenous avidin expression with an avidin/biotin complex according to the manufacturer's instructions. In addition, nonspecific binding was inhibited by preincubation with 5% goat serum. Sections were incubated overnight at 4°C with primary antibody diluted in 5% goat serum. Antibodies were as follows: vWF and IRF1 (as above); IRF8 (diluted 1:200; Abcam, ab28696); IFN-α (PBL Interferon Source, MMHA-2); IFN-β (diluted 1:100; PBL Interferon Source, MMHB-3). Negative controls were processed in parallel, except that 5% goat serum or an equivalent amount of normal mouse IgG (Santa Cruz) was substituted for the primary antibody. After washing 3 times, secondary antibody incubation was performed for

1 hour at room temperature using biotinylated goat anti-rabbit or goat anti-mouse IgG diluted 1:200 for all sections. HRP activity of biotin-labeled tissue antigens was achieved by incubation with ABC-HRP for 30 minutes, after which HRP activity was revealed with DAB for 30–90 seconds. Finally, sections were counterstained and mounted.

In vivo BrdU incorporation assay. After isoflurane anesthesia, 100 μl (10 mg/ml) of BrdU solution (BD Pharmingen) was injected into 3- to 4-week-old mice through the retro-orbital venous plexus. The mice were euthanized 1 hour after injection. BM cells were harvested, and BrdU staining was performed using APC BrdU Flow Kit (BD Pharmingen) following the manufacturer's instructions. Briefly, the BM cells were stained with CD41-FITC antibody and then fixed/permeabilized. After treatment with DNase, cells were stained with anti-BrdU APC antibody and 7-amino-actinomycin D (7AAD) and analyzed using a FACSCalibur flow cytometer (BD Biosciences).

In vivo IFN-α/β neutralizing antibody experiments. 4- to 6-week-old hemizygous male GATA1s mouse littermates (21) or WT C57BL/6 male mice were injected intraperitoneally with a combination of 1×10^4 neutralizing units each of polyclonal rabbit anti–IFN-α antibody (PBL InterferonSource, product no. 32100-1) and anti–IFN-β antibody (PBL InterferonSource, product no. 32400-1) or an equivalent amount (based on protein content) of normal rabbit IgG (Santa Cruz Biotechnologies, catalog no. sc-2027) in 200 μl sterile PBS. After 8 days, mice were euthanized, and BM cells were flushed from both femurs. After red blood cell lysis, cells were stained with anti-CD41–FITC (BD Pharmingen) (or anti-CD41–PE) following standard procedures and analyzed on a FACSCalibur flow cytometry instrument (BD Biosciences) with FlowJo software. vWF immunohistochemical staining was also performed on femoral BM sections, and the number of vWF^+ cells per 2-mm^2 field was counted in a blinded fashion.

Gene expression data. WT and GATA1s MkP cDNA microarray data have been deposited in GEO (accession nos. GSE45618 and GSE45619, respectively).

Statistics. GSEA statistical analysis was performed as previously described (43); a FDR of 0.25 or less and nominal *P* value of 0.01 or less was considered significant. 2-tailed Student's *t* test was used for all other statistical analyses; a *P* value of 0.05 or less was considered significant. All quantitative results show mean ± SEM.

Study approval. All human materials were collected according to protocols approved by Boston Children's Hospital Institutional Review Board (BM samples) and the Brigham and Women's Hospital Partners Human Research Committee (PHRC) (FL samples). Informed consent was not required since this was considered research on excess deidentified material collected for reasons other than research purposes. All experiments involving mice were approved by the Boston Children's Hospital Institutional Animal Care and Use Committee.

Acknowledgments

We thank Stuart Orkin for providing GATA1s mice, Genhong Cheng for providing *Ifnar1*$^{-/-}$ mice, Jonathan Keller for providing the Ifi205 (p205) antibody, Mark Fleming and Theonia Boyd for assisting with procurement of human BM and FL pathology specimens, and Andrei Kristov and Grigoriy Losyev for advice and assistance with cell sorting. We thank Zhe Li and Martha Sola-Visner for advice and critical review of the manuscript. This work was supported by grants from the German Academic Research Service (to K. Wieland), the NIH (R01 HL075705; to A.B. Cantor), and the American Society for Hematology (to A.B. Cantor).

Received for publication February 13, 2013, and accepted in revised form May 2, 2013.

Address correspondence to: Alan B. Cantor, 300 Longwood Ave., Karp 7, Children's Hospital Boston, Boston, Massachusetts 02115, USA. Phone: 617.919.2026; Fax: 617.730.0222; E-mail: alan.cantor@childrens.harvard.edu.

Andrew J. Woo's present address is: Western Australian Institute for Medical Research/Royal Perth Hospital, School of Medicine and Pharmacology, University of Western Australia, Perth, Australia.

Karen Wieland's present address is: Children's Hospital, Technical University Munich, Munich, Germany.

1. Zipursky A, Peeters M, Poon A. Megakaryoblastic leukemia and Down's syndrome: a review. *Pediatr Hematol Oncol*. 1987;4(3):211–230.
2. Robison LL. Down syndrome and leukemia. *Leukemia*. 1992;6(Suppl. 1):5–7.
3. Avet-Loiseau H, Mechinaud F, Harousseau JL. Clonal hematologic disorders in Down syndrome. A review. *J Pediatr Hematol Oncol*. 1995;17(1):19–24.
4. Zipursky A, Brown EJ, Christensen H, Doyle J. Transient myeloproliferative disorder (transient leukemia) and hematologic manifestations of Down syndrome. *Clin Lab Med*. 1999;19(1):157–167, vii.
5. Langebrake C, Creutzig U, Reinhardt D. Immunophenotype of Down syndrome acute myeloid leukemia and transient myeloproliferative disease differs significantly from other diseases with morphologically identical or similar blasts. *Klin Padiatr*. 2005; 217(3):126–134.
6. Bourquin JP, et al. Identification of distinct molecular phenotypes in acute megakaryoblastic leukemia by gene expression profiling. *Proc Natl Acad Sci U S A*. 2006;103(9):3339–3344.
7. Ito E, et al. Expression of erythroid-specific genes in acute megakaryoblastic leukaemia and transient myeloproliferative disorder in Down's syndrome. *Br J Haematol*. 1995;90(3):607–614.
8. Massey GV, et al. A prospective study of the natural history of transient leukemia (TL) in neonates with Down syndrome (DS): Children's Oncology Group (COG) study POG-9481. *Blood*. 2006; 107(12):4606–4613.
9. Klusmann JH, et al. Treatment and prognostic impact of transient leukemia in neonates with Down syndrome. *Blood*. 2008;111(6):2991–2998.
10. Wechsler J, et al. Acquired mutations in GATA1 in the megakaryoblastic leukemia of Down syndrome. *Nat Genet*. 2002;32(1):148–152.
11. Mundschau G, Gurbuxani S, Gamis AS, Greene ME, Arceci RJ, Crispino JD. Mutagenesis of GATA1 is an initiating event in Down syndrome leukemogenesis. *Blood*. 2003;101(11):4298–4300.
12. Hitzler JK, Cheung J, Li Y, Scherer SW, Zipursky A. GATA1 mutations in transient leukemia and acute megakaryoblastic leukemia of Down syndrome. *Blood*. 2003;101(11):4301–4304.
13. Ahmed M, et al. Natural history of GATA1 mutations in Down syndrome. *Blood*. 2004;103(7):2480–2489.
14. Groet J, et al. Acquired mutations in GATA1 in neonates with Down's syndrome with transient myeloid disorder. *Lancet*. 2003;361(9369):1617–1620.
15. Rainis L, et al. Mutations in exon 2 of GATA1 are early events in megakaryocytic malignancies associated with trisomy 21. *Blood*. 2003;102(3):981–986.
16. Shivdasani RA, Fujiwara Y, McDevitt MA, Orkin SH. A lineage-selective knockout establishes the critical role of transcription factor GATA-1 in megakaryocyte growth and platelet development. *EMBO J*. 1997;16(13):3965–3973.
17. Vyas P, Ault K, Jackson CW, Orkin SH, Shivdasani RA. Consequences of GATA-1 deficiency in megakaryocytes and platelets. *Blood*. 1999;93(9):2867–2875.
18. Harigae H, Xu G, Sugawara T, Ishikawa I, Toki T, Ito E. The GATA1 mutation in an adult patient with acute megakaryoblastic leukemia not accompanying Down syndrome. *Blood*. 2004;103(8):3242–3243.
19. Hollanda LM, et al. An inherited mutation leading to production of only the short isoform of GATA-1 is associated with impaired erythropoiesis. *Nat Genet*. 2006;38(7):807–812.
20. Sankaran VG, et al. Exome sequencing identifies GATA1 mutations resulting in Diamond-Blackfan anemia. *J Clin Invest*. 2012;122(7):2439–2443.
21. Li Z, Godinho FJ, Klusmann JH, Garriga-Canut M, Yu C, Orkin SH. Developmental stage-selective effect of somatically mutated leukemogenic transcription factor GATA1. *Nat Genet*. 2005; 37(6):613–619.
22. Pronk CJ, et al. Elucidation of the phenotypic, functional, and molecular topography of a myeloerythroid progenitor cell hierarchy. *Cell Stem Cell*. 2007; 1(4):428–442.
23. Wang Q, Miyakawa Y, Fox N, Kaushansky K. Interferon-alpha directly represses megakaryopoiesis by inhibiting thrombopoietin-induced signaling through induction of SOCS-1. *Blood*. 2000; 96(6):2093–2099.
24. Kiladjian JJ, et al. Pegylated interferon-alfa-2a induces complete hematologic and molecular responses with low toxicity in polycythemia vera. *Blood*. 2008;112(8):3065–3072.
25. Abegg-Werter MJ, Raemaekers JM, de Pauw BE, Haanen C. Recombinant interferon-alpha, but not interferon-gamma is effective therapy for essential

thrombocythemia. *Blut*. 1990;60(1):37–40.
26. Kujawski LA, Talpaz M. The role of interferon-alpha in the treatment of chronic myeloid leukemia. *Cytokine Growth Factor Rev*. 2007;18(5–6):459–471.
27. Muller U, et al. Functional role of type I and type II interferons in antiviral defense. *Science*. 1994; 264(5167):1918–1921.
28. Negrotto S, et al. Expression and functionality of type I interferon receptor in the megakaryocytic lineage. *J Thromb Haemost*. 2011;9(12):2477–2485.
29. Xu J, et al. Combinatorial assembly of developmental stage-specific enhancers controls gene expression programs during human erythropoiesis. *Dev Cell*. 2012;23(4):796–811.
30. Matsuyama T, et al. Targeted disruption of IRF-1 or IRF-2 results in abnormal type I IFN gene induction and aberrant lymphocyte development. *Cell*. 1993;75(1):83–97.
31. Essers MA, et al. IFNα activates dormant haematopoietic stem cells in vivo. *Nature*. 2009; 458(7240):904–908.
32. Klimmeck D, Hansson J, Raffel S, Vakhrushev SY, Trumpp A, Krijgsveld J. Proteomic cornerstones of hematopoietic stem cell differentiation: distinct signatures of multipotent progenitors and myeloid committed cells. *Mol Cell Proteomics*. 2012; 11(8):286–302.
33. Nakamura K, Deyama Y, Yoshimura Y, Suzuki K, Morita M. Toll-like receptor 3 ligand-induced antiviral response in mouse osteoblastic cells. *Int J Mol Med*. 2007;19(5):771–775.
34. Takayanagi H, et al. RANKL maintains bone homeostasis through c-Fos-dependent induction of interferon-β. *Nature*. 2002;416(6882):744–749.
35. Darnell JE Jr, Kerr IM, Stark GR. Jak-STAT pathways and transcriptional activation in response to IFNs and other extracellular signaling proteins. *Science*. 1994;264(5164):1415–1421.
36. Li X, Leung S, Qureshi S, Darnell JE Jr, Stark GR. Formation of STAT1-STAT2 heterodimers and their role in the activation of IRF-1 gene transcription by interferon-α. *J Biol Chem*. 1996; 271(10):5790–5794.
37. Muntean AG, Crispino JD. Differential requirements for the activation domain and FOG-interaction surface of GATA-1 in megakaryocyte gene expression and development. *Blood*. 2005; 106(4):1223–1231.
38. Huang Z, Richmond TD, Muntean AG, Barber DL, Weiss MJ, Crispino JD. STAT1 promotes megakaryopoiesis downstream of GATA-1 in mice. *J Clin Invest*. 2007;117(12):3890–3899.
39. Klusmann JH, et al. Developmental stage-specific interplay of GATA1 and IGF signaling in fetal megakaryopoiesis and leukemogenesis. *Genes Deve*. 2010; 24(15):1659–1672.
40. Liu ZJ, Sola-Visner M. Neonatal and adult megakaryopoiesis. *Curr Opin Hematol*. 2011;18(5):330–337.
41. Silver RT, Vandris K, Goldman JJ. Recombinant interferon-α may retard progression of early primary myelofibrosis: a preliminary report. *Blood*. 2011; 117(24):6669–6672.
42. Liu T, et al. Cistrome: an integrative platform for transcriptional regulation studies. *Genome Biol*. 2011;12(8):R83.
43. Subramanian A, et al. Gene set enrichment analysis: a knowledge-based approach for interpreting genome-wide expression profiles. *Proc Natl Acad Sci U S A*. 2005;102(43):15545–15550.
44. Radaeva S, et al. Interferon-α activates multiple STAT signals and down-regulates c-Met in primary human hepatocytes. *Gastroenterology*. 2002; 122(4):1020–1034.
45. Browne EP, Wing B, Coleman D, Shenk T. Altered cellular mRNA levels in human cytomegalovirus-infected fibroblasts: viral block to the accumulation of antiviral mRNAs. *J Virol*. 2001; 75(24):12319–12330.